

AD-A192 711

BULK PLASMON ENHANCED PHOTOEMISSION FROM Nb(100)
SURFACE RESONANCES(U) TEXAS UNIV AT AUSTIN DEPT OF
PHYSICS B S FANG ET AL 08 APR 88 AFOSR-TR-88-0426

1/1

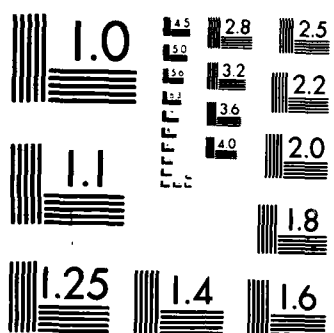
UNCLASSIFIED

AFOSR-86-0109

F/G 20/12

NL





2

Form Approved
OMB No. 0704-0188

AD-A192 711

DOCUMENTATION PAGE

1b. RESTRICTIVE MARKINGS
None DTIC FILE COPY

2a. SECURITY CLASSIFICATION AUTHORITY

2b. DECLASSIFICATION/DOWNGRADING SCHEDULE

3. DISTRIBUTION/AVAILABILITY OF REPORT
Approved for public release;
Distribution unlimited

4. PERFORMING ORGANIZATION REPORT NUMBER(S)

5. MONITORING ORGANIZATION REPORT NUMBER(S)

AFOSR-TK- 88 - 0426

6a. NAME OF PERFORMING ORGANIZATION
The University of Texas
Department of Physics

6b. OFFICE SYMBOL
(If applicable)

7a. NAME OF MONITORING ORGANIZATION
Air Force Office of Scientific Research
Chemical and Atmospheric Sciences

6c. ADDRESS (City, State, and ZIP Code)
The University of Texas at Austin
Department of Physics
Austin, Texas 78712

7b. ADDRESS (City, State, and ZIP Code)
Building 410
Bolling Air Force Base
Washington, D.C. 20332-6448

8a. NAME OF FUNDING/SPONSORING
ORGANIZATION
AFOSR

8b. OFFICE SYMBOL
(If applicable)
NC

9. PROCUREMENT INSTRUMENT IDENTIFICATION NUMBER
AFOSR-86-0109

8c. ADDRESS (City, State, and ZIP Code)
Building 410
Bolling AFB, DC 20332-6448

10. SOURCE OF FUNDING NUMBERS
PROGRAM ELEMENT NO. 61102F PROJECT NO. 2303 TASK NO. A2 WORK UNIT ACCESSION NO.

11. TITLE (Include Security Classification)
Bulk plasmon enhanced photoemission from Nb(100) surface resonances.

12. PERSONAL AUTHOR(S)
B.-S. Fang, C.A. Ballentine, and J.L. Erskine

13a. TYPE OF REPORT
Reprint

13b. TIME COVERED
FROM 1/1/87 TO 3/31/88

14. DATE OF REPORT (Year, Month, Day)
88/04/08

15. PAGE COUNT
16

16. SUPPLEMENTARY NOTATION

17. COSATI CODES
FIELD GROUP SUB-GROUP

18. SUBJECT TERMS (Continue on reverse if necessary and identify by block number)

19. ABSTRACT (Continue on reverse if necessary and identify by block number)

The electronic properties of Nb(100) are studied using angle-resolved photoemission. Several surface resonances are identified. One surface resonance exhibits significant enhancement of the photoemission cross section at the bulk plasma energy suggesting a novel probe of surface resonances having high degree of second-layer charge density.

DTIC
ELECTE
MAY 02 1988
S D

20. DISTRIBUTION/AVAILABILITY OF ABSTRACT
☒ UNCLASSIFIED/UNLIMITED ☐ SAME AS RPT. ☐ DTIC USERS

21. ABSTRACT SECURITY CLASSIFICATION
Unclassified/Unlimited

22a. NAME OF RESPONSIBLE INDIVIDUAL
Lt. Col. Larry Burggraf

22b. TELEPHONE (Include Area Code)
(202) 767-4960

22c. OFFICE SYMBOL
NC

Bulk plasmon enhanced photoemission from Nb(100)
surface resonances

B.-S. Fang, C.A. Ballentine, and J.L. Erskine
Department of Physics
University of Texas
Austin, Texas 78712

The electronic properties of Nb(100) are studied using angle-resolved photoemission. Several surface resonances are identified. One surface resonance exhibits significant enhancement of the photoemission cross section at the bulk plasma energy suggesting a novel probe of surface resonances having high degree of second-layer charge density.

Accession For	
NTIS GRA&I	<input checked="" type="checkbox"/>
DTIC TAB	<input type="checkbox"/>
Unannounced	<input type="checkbox"/>
Justification	
By	
Distribution/	
Availability Codes	
Dist	Avail and/or Special
A-1	

PAX 79.60.c clean metal (photoemission)

73.20 surface electronic state

88 5 02 132

Approved for public release;
distribution unlimited.

We report the observation of bulk plasmon enhanced photoemission from Nb(100) surface resonances. This effect offers a sensitive direct probe of the spatial extent of surface states and surface resonances at metal surfaces in cases where a high degree of second-layer charge density exists in the two-dimensional Brillouin zone. A related enhancement effect has been recently reported by Drube and Himpfel¹ for inverse photoemission. Photoemission cross section resonances associated with surface states which arise from final-state effects have also been observed on ^{Silver}Ag(111)² and ^{Copper}Cu(111)³ surfaces. However, these resonances are produced by a distinctly different mechanism than the one described in this paper.

Intrinsic surface properties appear to play an important role in the kinetic behavior of the H/Nb(100) system. Our experiments on Nb(100) were motivated by recent studies of the H/Nb(100) system^{4,5} that have yielded experimental evidence for subsurface hydrogen sites which exhibit novel reversible temperature dependent properties. These hydrogen states appear to govern up-take kinetics of hydrogen at Nb surfaces as well as the admission of hydrogen into the bulk.⁶ The present work deals primarily with the electronic properties of the clean Nb(100) surface.

Niobium is a bcc Group VB transition metal having bulk electronic properties very similar to Mo and W which are also bcc transition metals. We first review some of the electronic properties of Mo(100) and W(100) obtained by Weng, Plummer, and Gustafsson⁷, because we have found the properties of Nb(100) to be very similar. The Mo and W results serve as a guide to our analysis of Nb(100) electronic properties. We also summarize the available electronic structure models for Nb(100)⁸. Mo(100) and W(100) exhibit three occupied surface resonance bands which exist

throughout the two-dimensional Brillouin zone. The resonances are located at approximately 0.2, 0.6, and 3.3 and (0.3, 0.8, and 4.2) eV below the Fermi energy (E_F) for Mo (W). In normal emission ($k_{\parallel}=0$), only one of the two higher lying resonances and the low lying resonance are observed on both Mo(100) and W(100). The symmetry of both states observed at $k_{\parallel}=0$ is Δ_1 (dz^2). The k_{\parallel} dispersion of all three surface resonances is small < 0.3 eV. Two higher lying states are observed on both Mo(100) and W(100) for $k_{\parallel}\neq 0$. The two higher lying resonances have different character based on the cross section dependence on polarization.

Louie et al.⁸ have reported self-consistent pseudopotential calculations for the ideal Nb(100) surface. The surface bands exhibit a number of gaps in the projected bulk bands, primarily around \bar{M} and along the $\bar{M} - \bar{X}$ direction. There are several symmetry gaps at $\bar{\Gamma}$. Prominent surface states are predicted to exist in absolute gaps at \bar{X} and \bar{M} , and a number of resonances are predicted to lie in the symmetry gaps throughout the two-dimensional Brillouin zone. Specific predictions pertaining to observed surface resonances are described later in relation to our experimental data.

Our experiments were performed at the Synchrotron Radiation Center, Stoughton, Wisconsin, using a photoelectron spectrometer which has been described previously⁴. The single crystal samples were prepared using conventional methods^{4,5} and characterized using Auger Spectroscopy and low energy electron diffraction (LEED). Fig.1 displays selected angle-resolved energy distribution curves (EDC's) for Nb(100) obtained using normal emission geometry. Light was incident at $\theta_I=45^\circ$ with

polarization vector E along a (10) crystal axis. Three prominent structures in the EDC's are designated by Δ_1 , $\bar{\Delta}_1$ and $\bar{\Delta}_1'$. We first establish the origin of these peaks, and obtain an accurate set of bulk Nb bands.

Peak binding energy shifts in EDC's as a function photon energy at fixed $k_{//}$ are characteristic of direct transitions between bulk electronic states. The peak labeled Δ_1 is produced by emission from the lower Δ_1 symmetry bulk band of Nb. Fig. 2 illustrates the bulk band structure of Nb calculated by Louie, Ho and Cohen⁹. Final bands lying more than 6eV above E_F have been adapted from the calculated band structure of Mo¹⁰. Energy bands and critical point energies of the final bands above E_F have been adjusted to fit our experimental results for the upper Δ_1 symmetry band. These adjustments yield final bands in excellent agreement with photoemission data from Smith et al.¹¹ and inverse photoemission data from Johnson¹² for Nb(110). It is clear from Fig. 2 that the peaks labeled Δ_1 originate from the lower Δ_1 bulk band. All of the experimental data (both photoemission and inverse photoemission) appears to yield results that are consistent with the band model of Fig. 2. We, therefore, judge this model an accurate representation of the excitation energies of bulk states in Nb.

The other two structures labeled $\bar{\Delta}_1$ and $\bar{\Delta}_1'$ are attributed to surface resonances. The binding energies of these two structures do not vary with photon energy, showing that they can be assigned two-dimensional character, and both peaks are more sensitive to hydrogen adsorption than the bulk state feature as shown by EDC's taken after exposing the clean

Nb(100) surface to 1-2 Langmuirs of H_2 (refer to the lower EDC of Fig. 1 and ref. 4). The surface sensitivity of the two higher lying peaks also supports assigning them to surface states or surface resonances.

Careful inspection of the spectra in Fig. 1 reveals an easily resolved but small binding energy shift in the $\bar{\Delta}'_1$ peak as a function of photon energy. Hydrogen exposure also induces peak shifts of a similar magnitude⁴ (0.1 – 0.2 eV). These effects suggest that at least two states contribute to the $\bar{\Delta}'_1$ structure. We have considered two possibilities to account for the multiple contributions: The first possibility is based on contributions from the bulk state at $\Gamma_{25'}$ and one or more surface resonances. The second possibility is based on contributions from two different surface resonances as Weng et al. found for Mo(100) and W(100). Shore and Papconstantopoulous¹³ have recently studied the transferability of Slater-Koster parameters in transition metals and have shown that the position of the Fermi energy is a sensitive function of these parameters. Niobium was used specifically to demonstrate this sensitivity and based on the results, it is not unreasonable to assume the possibility of an error of the order of one hundred meV in the placement of E_F for calculated bands. In Nb, small errors in E_F can make the difference in whether the Γ_{25} point lies above or partly below E_F . Most calculations^{10,14} place the Δ_5 band just above E_F . These calculations are consistent with Fermi surface properties. Fermi surface measurements have not necessarily detected the small occupied portion of the Σ_1 band which is believed to occur about half way between Γ and N of the three-dimensional Brillouin

zone. The photoemission experiments of Smith et al.¹¹ on Nb(110) have yielded some evidence that part of the lower Σ_1 band is filled. This result clearly places Γ'_{25} above E_F . There is also the possibility that band tailing at Γ resulting from finite temperature contributes to the structure at E_F . We prefer to attribute the observed behavior to a pair of different surface resonances as observed on the (100) surfaces of Mo and W. However, the primary result of this paper does not depend on the precise placement of E_F relative to the lower Δ_5 band.

The peaks labeled $\overline{\Delta}_1$ and $\overline{\Delta}'_1$ result from surface states or surface resonances. Therefore their binding energies must lie in real gaps or symmetry gaps of the projected bulk states. Fig. 3 illustrates Louie et al.'s⁸ calculated surface bands and projected bulk bands for Nb(100). At $\overline{\Gamma}$, a surface state of $d_{3z^2-r^2}$ character is found in a $\overline{\Gamma}_1$ symmetry gap 0.2 eV above E_F . Also found near E_F is an unoccupied surface band in a $\overline{\Delta}_1$ symmetry gap, and an occupied band of strong surface resonances lying just below E_F . The experimental data of Fig. 3 is consistent with these predictions. Off-normal spectra for Nb(100) exhibit splitting of the high lying peak near E_F that we attribute to a pair of surface resonances⁴. The projected bulk bands (Fig. 3) show that the even state symmetry gap at $\overline{\Gamma}$ extends from near E_F to approximately 2.5 eV below E_F . Although no strong surface resonances were predicted 2.5 eV below E_F at $\overline{\Gamma}$, the gap permits a $\overline{\Delta}_1$ symmetry surface resonance to exist at $\overline{\Gamma}$ as our data suggests.

The above discussion serves to establish the origin of the three peaks, and to show that the peak assignments are consistent with available calculations. Our results are also in general agreement with corresponding experimental data for Mo(100) and W(100). We now turn to the photoemission enhancement of the lower surface resonance cross section.

Examination of Fig. 1 reveals that the lower $\bar{\Delta}_1$ surface resonance cross section is a maximum for $h\nu \cong 23\text{eV}$. This enhanced cross section can not be attributed to a final state effect.² Resonances in the surface-state photoemission cross section can occur at photon energies corresponding to direct transitions from the surface state to regions of final bulk bands described by Bloch States^{2,3} that exhibit a high density of states (i.e., at the zone center or at zone boundaries). It is important to note that models that account for these final state resonances require that the decay length of the surface state or surface resonance into the bulk is long compared to the crystal interlayer spacing. According to Fig. 2, final state resonances for the lower $\bar{\Delta}_1$ state could be expected to occur at photon energies corresponding to transitions to the upper Γ_1 state ($h\nu=25.8\text{eV}$) or to the upper H_{12} state ($h\nu=16\text{eV}$). The observed maximum in the Δ_1 surface resonance cross section occurs between these photon energies (at $h\nu \cong 23\text{eV}$). Note that the bulk Δ_1 state cross section is also maximum at $h\nu \cong 23\text{eV}$, and final state resonances for this band should occur at $h\nu \cong 29.5\text{eV}(\Gamma)$ or $h\nu=26.7\text{eV}(H)$. We therefore can not attribute the enhancement in cross section of the $\bar{\Delta}_1$ surface resonance emission or the

Δ_1 bulk state emission, to a final state resonance. The bulk plasma resonance for Nb occurs at $h\nu \approx 23\text{eV}$, and below, we present a mechanism that accounts for the cross section enhancement of both states based on this resonance.

Fig. 4 presents the photon energy dependence of the emission cross sections for the bulk (Δ_1) peak, the $\bar{\Delta}_1$ surface resonance peak, and the $\bar{\Delta}'_1$ surface resonance. Note that the cross sections associated with the bulk peak and lower $\bar{\Delta}_1$ resonance are similar while the higher lying $\bar{\Delta}'_1$ resonance cross section is qualitatively different. The cross section energy dependence of all three states can be explained by considering the photon energy dependence of the normal component of the electric field, E_z , just above and just below the surface (also illustrated in Fig. 4). Based on symmetry selection rules, it is the Z component of the electric field that causes the $\Delta_1 \rightarrow \Delta_1$ bulk interband transitions, and $\bar{\Delta}_1$ (even symmetry) transitions at $\bar{\Gamma}$ of the two-dimensional Brillouin zone. Optical constants from Weaver et al.¹⁵ were used to calculate the electric field strength just above the surface, and just below the surface based on the Fresnel formulas from Jackson¹⁶. The behavior, illustrated in Fig. 4, is similar to what Weng et al. obtained for Mo and W, and is characteristic of all metals near the bulk plasma frequency: The normal component of the electric field just above the surface experiences a local minimum as $h\nu$ passes through the plasma frequency, ω_p . The corresponding field inside the surface experiences a local maximum just above ω_p . Based on this effect, bulk states and surface resonances which have charge density extending beyond the surface should experience enhanced cross sections

just above ω_p . True surface (top layer) resonances can be expected to experience suppressed cross sections at $h\nu \approx \omega_p$ as shown by the calculated results in Fig. 4. and the spectra for the $\bar{\Delta}'_1$ surface resonance. In discussing their calculations of the surface resonances on Nb(100) Louie et al.⁸ noted that several of the surface resonance bands (the T_5 and T_4 bands in particular) exhibit a striking change in character over different regions of k space. In some regions of k space, the concentration of charge is shifted from the first (surface) layer to the second layer. Unfortunately, our experiments did not probe the line in k space extending from \bar{X} to \bar{M} where these effects are predicted to exist. However, our results presented for states around $\bar{\Gamma}$ represent a reasonably good endorsement of the accuracy of the surface calculations as well as a demonstration of a novel probe of the depth that a resonance penetrates into the surface based on bulk plasma assisted processes. The clear implication of our results is that the lower $\bar{\Delta}_1$ surface resonance extends into the bulk while the upper $\bar{\Delta}'_1$ resonance is highly localized at the surface. The latter conclusion is not unreasonable. If the Γ'_{25} point lies above E_F as, predicted by first-principals calculations, the upper $\bar{\Delta}_1$ band may lie below the projected Σ_1 and Δ_5 bulk bands, and can therefore be considered a true surface state.

We wish to thank the staff of the Synchrotron Radiation Center for their assistance in conducting these experiments, and P.D. Johnson for providing inverse photoemission results prior to publication. This work was

supported by NSF/DMR 8702848, AFOSR-86-0109, and the Robert A. Welch Foundation. The Synchrotron Radiation Center in Stoughton, Wisconsin is supported by NSF.

REFERENCES

1. W. Drube and F.J. Himpsel, *Phys. Rev. Lett.* **60**, 140 (1988).
2. T.C. Hsieh, P. John, T. Miller, and T.-C. Chiang, *Phys. Rev.* **B35**, 3728 (1987).
3. S.G. Louie, P. Thiry, R. Pinchaux, Y. Petroff, D. Chandesris, and J. Lecante, *Phys. Rev. Lett.* **44**, 549 (1980).
4. B.-S. Fang, C.A. Ballentine, and J.L. Erskine, *Phys. Rev.* **B36**, 7360 (1987).
5. Y.Li, J.L. Erskine, and A.C. Diebold, *Phys. Rev.* **B34**, 5951 (1986).
6. M. Lagos and I.K. Schuller, *Phys. Rev.* **B32**, 5477 (1985); G.J. Dienes, M. Strongin, and D.O. Welch, *Phys. Rev.* **B34**, 5475 (1985).
7. S.-L. Weng, E.W. Plummer, and T. Gustafsson, *Phys. Rev.* **B18**, 1718 (1978).
8. S.G. Louie, K.-M. Ho, J.R. Chelikowsky, and M.L. Cohen, *Phys. Rev.* **B15**,

5622 (1977).

9. S.G. Louie, K.-M. Ho, and M.L. Cohen, *Phys. Rev.* **B19**, 1774 (1979).

10. A. Zunger, G.P. Kerker, and M.L. Cohen, *Phys. Rev.* **B20**, 581 (1979).

11. R.J. Smith, G.P. Williams, J. Colbert, M. Sagurton, and G.J. Lapeyre, *Phys. Rev.* **B22**, 1584 (1980).

12. P.D. Johnson (private communication).

13. J.D. Shore and D.A. Papaconstantopoulos, *Phys. Rev.* **B35**, 1122 (1987).

14. L.F. Mattheiss, *Phys. Rev.* **B1**, 373 (1970); J.R. Anderson, D.A. Papaconstantopoulos, J.W. Mc Caffrey, and J.E. Schirber, *Phys. Rev.* **B7**, 5115 (1973).

15. J.H. Weaver, D.W. Lynch, and C.G. Olsen, *Phys. Rev.* **B7**, 4311 (1973).

16. J.D. Jackson, *Classical Electrodynamics*, Second edition, John Wiley & Sons, Inc., N.Y. (p. 278).

FIGURE CAPTIONS

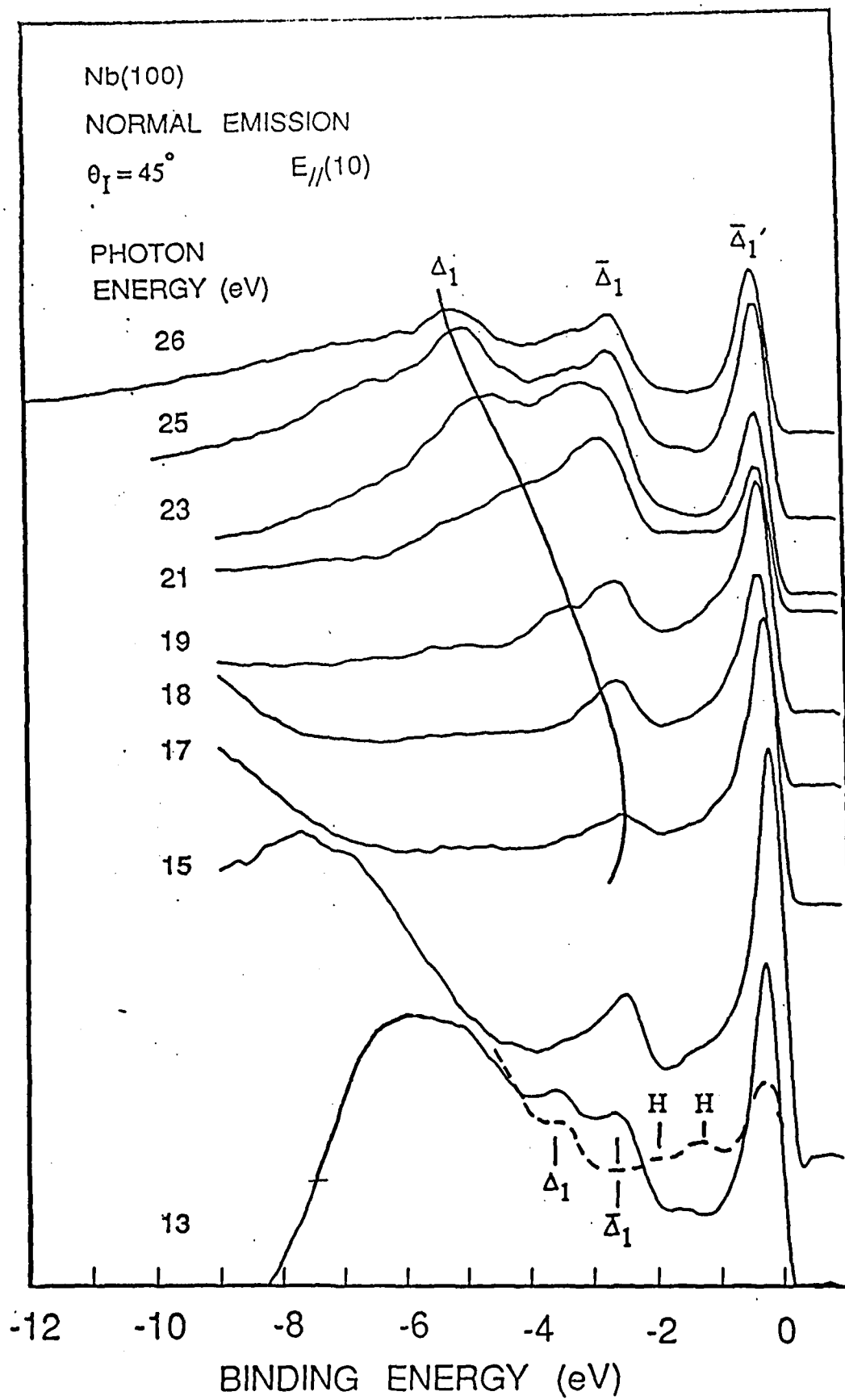
Fig. 1 Normal emission ($k_{\parallel} = 0$) electron energy distribution curves (EDC's) for Nb(100). The dashed line labeled Δ_1 shows the dispersion of the lower Δ_1 bulk state. The peaks labeled $\bar{\Delta}_1$ and $\bar{\Delta}'_1$ are produced by surface resonances at $\bar{\Gamma}$. Lower EDC (dotted line) illustrates the effect of 2.2L H_2 on Nb(100) at $h\nu=13\text{eV}$.

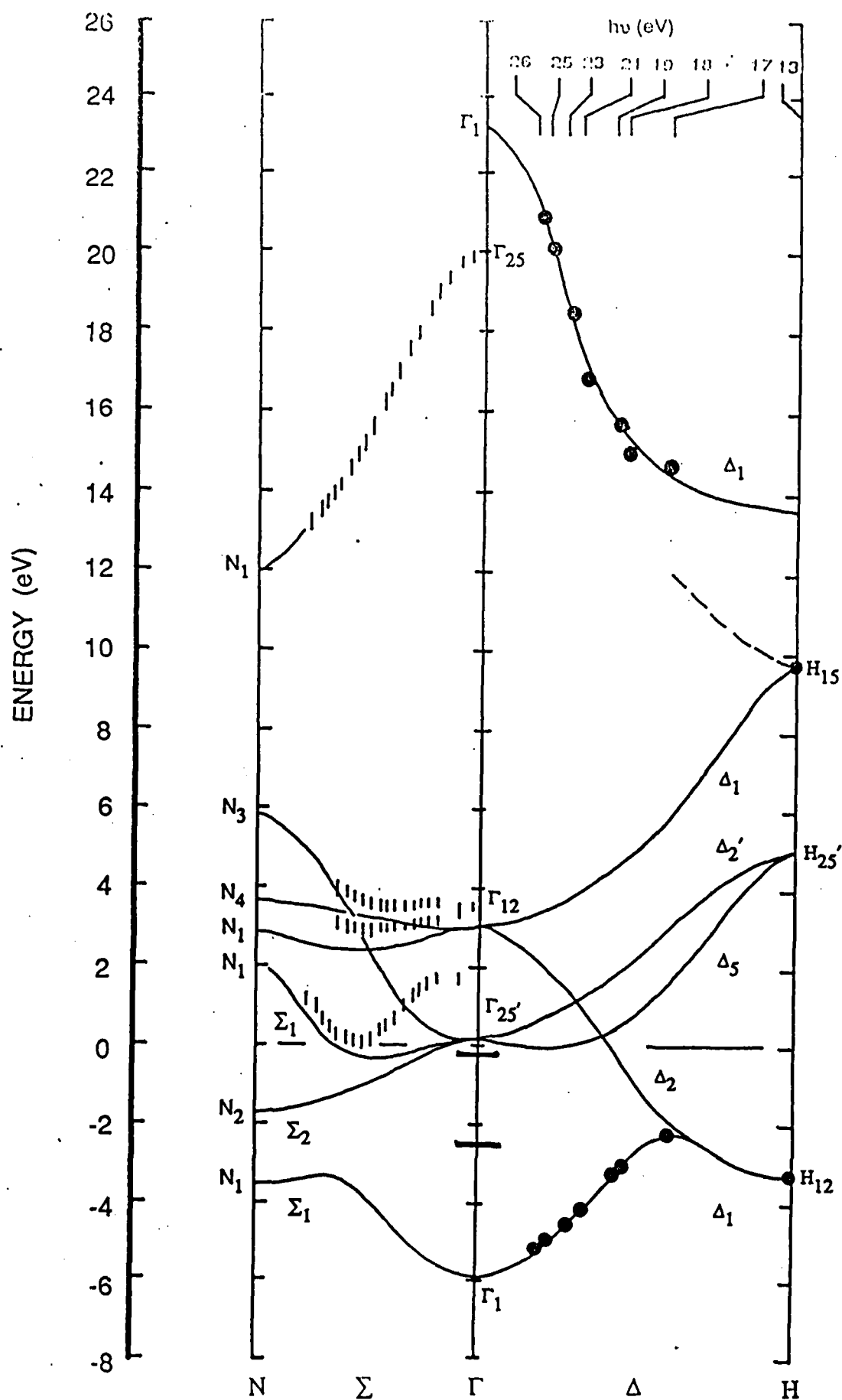
Fig. 2 Bulk band structure of Nb calculated by Louie et al. (ref. 8). Dots illustrate peak positions of the lower Δ_1 state established by experimental data of Fig. 1, and the corresponding Δ_1 symmetry final state energies. Vertical bars along the Σ direction show final bands above E_F established by inverse photoemission (ref. 12). Bars at 0.2eV (-2.3eV) (Γ point) shows location of upper (lower) surface resonance.

Fig. 3 Projected bulk bands of Nb(100) from Louie et al. (ref. 9). The lower surface resonance lies near the (even state) symmetry gap at Γ of the two-dimensional Brillouin zone.

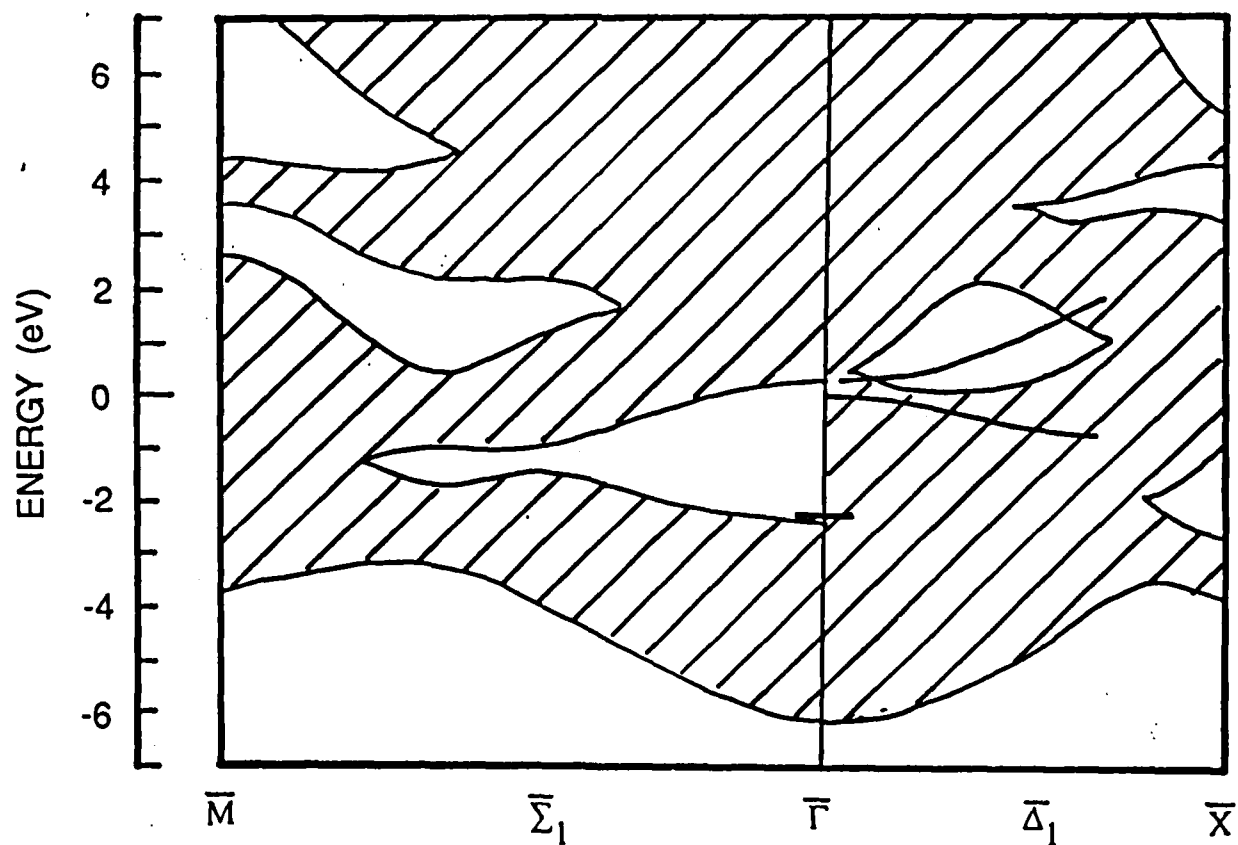
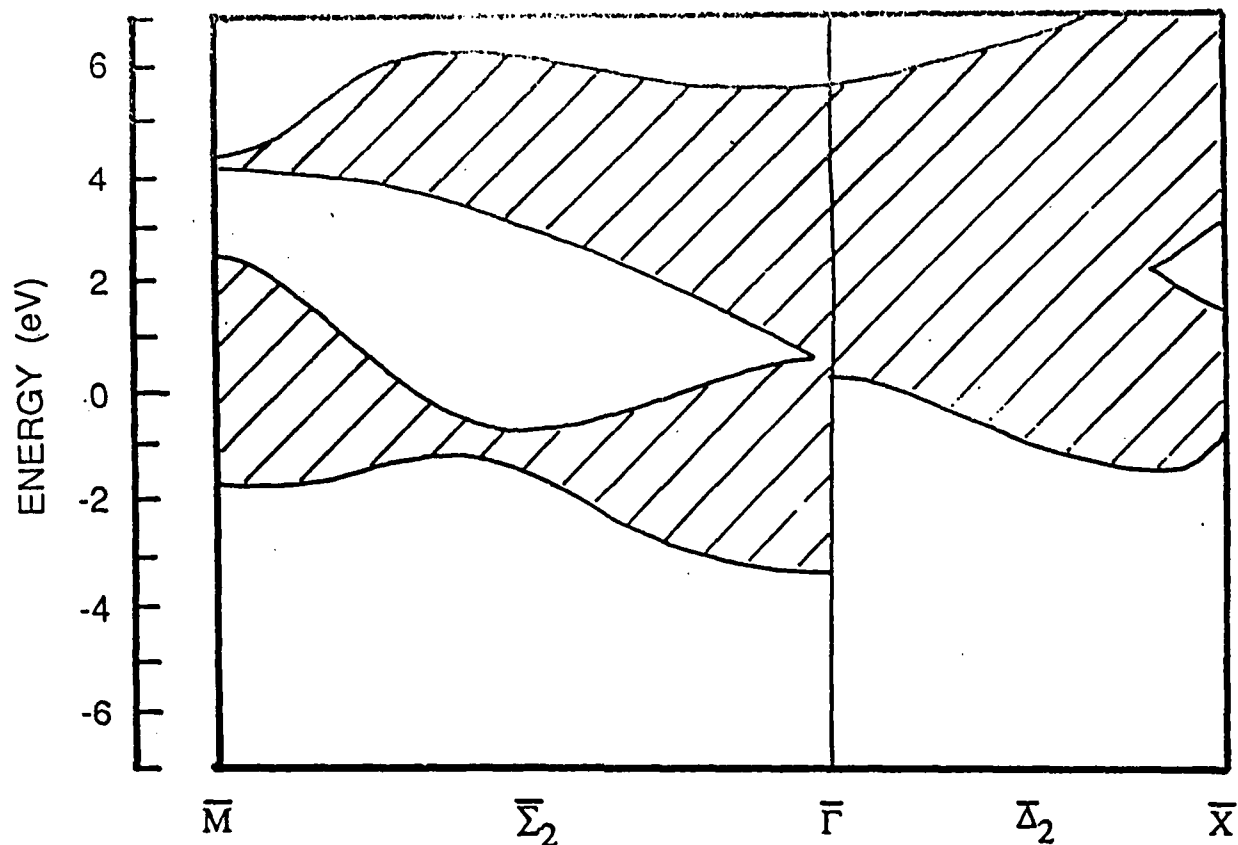
Fig. 4 Upper panel displays energy dependence of the photoemission cross section for the bulk state (Δ_1) and the two Δ_1 symmetry surface resonances. Lower panel displays calculated electric field strength normal to the surface just above ($|E_{\parallel}|^2$ out) and just below ($|E_{\parallel}|^2$ in) the surface for light incident at 45° from the surface normal direction.

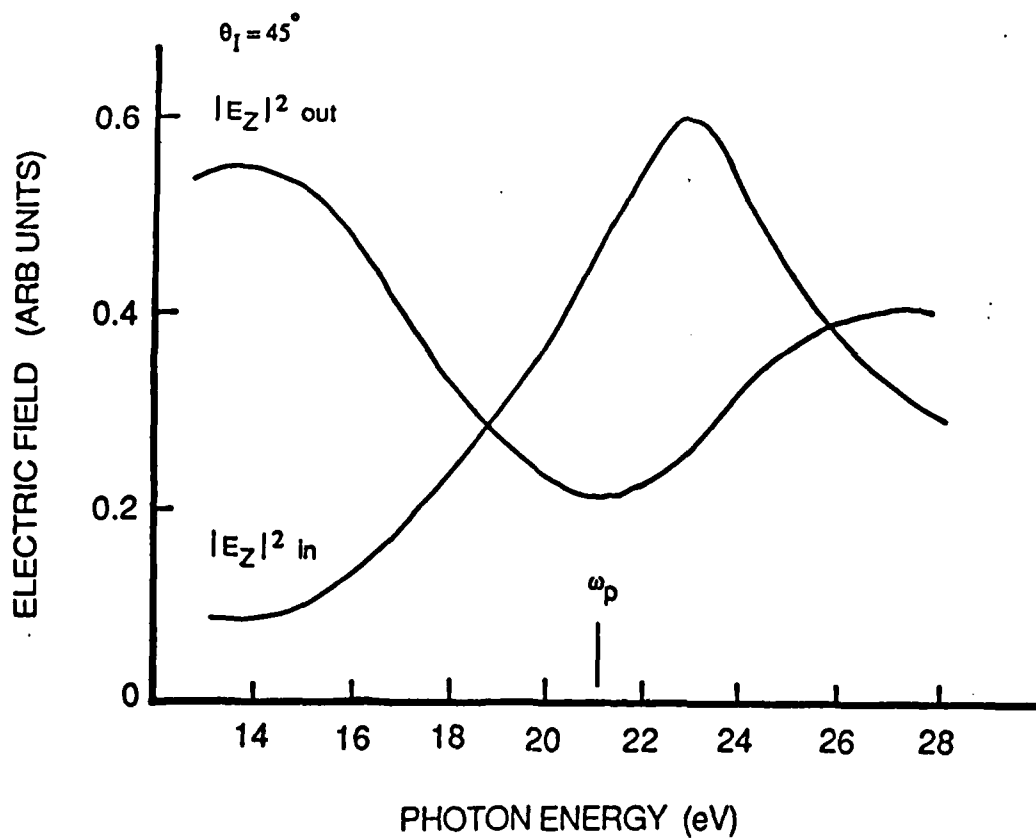
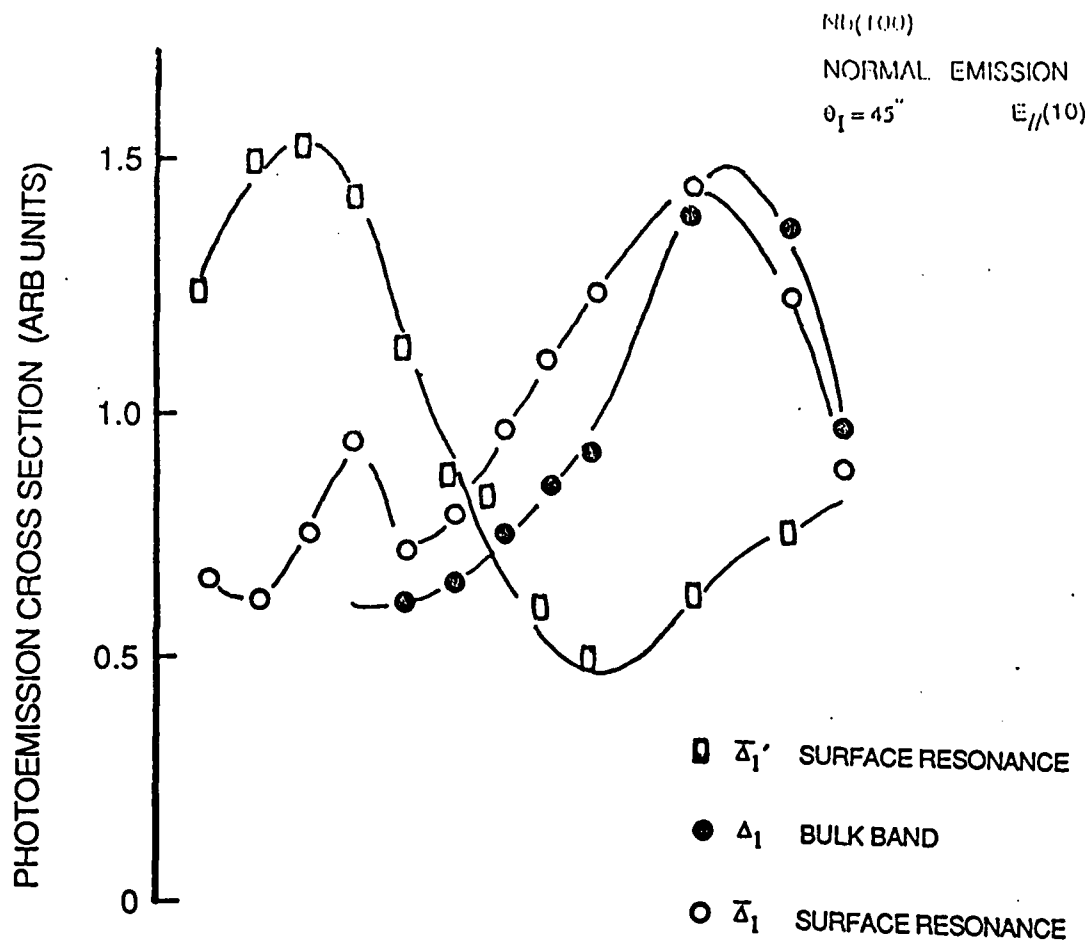
PHOTOEMISSION INTENSITY (ARB. UNITS)





Nb(100)





END

DATE

FILMED

6-88

DTIC